New Carbon Materials, 2024, 39(1): 131-141

Supporting Information

Bismuth nanoparticles anchored on N-doped graphite felts to give stable and efficient iron-chromium redox flow batteries

Hang-xin Che[1], Yu-fei Gao[2], Jia-hui Yang[1], Song Hong[1,*], Lei-duan Hao[1], Liang Xu[1], Sana Taimoor[1], Alex W. Robertson[3], Zhen-yu Sun[1,*]

[1]State Key Laboratory of Organic-Inorganic Composites, College of Chemical Engineering, Beijing University of Chemical Technology, Beijing 100029, China

[2]School of Mechanical and Electrical Engineering, Guilin University of Electronic Technology, Guilin 541004, China

[3]Department of Physics, University of Warwick, Coventry CV4 7AL, UK

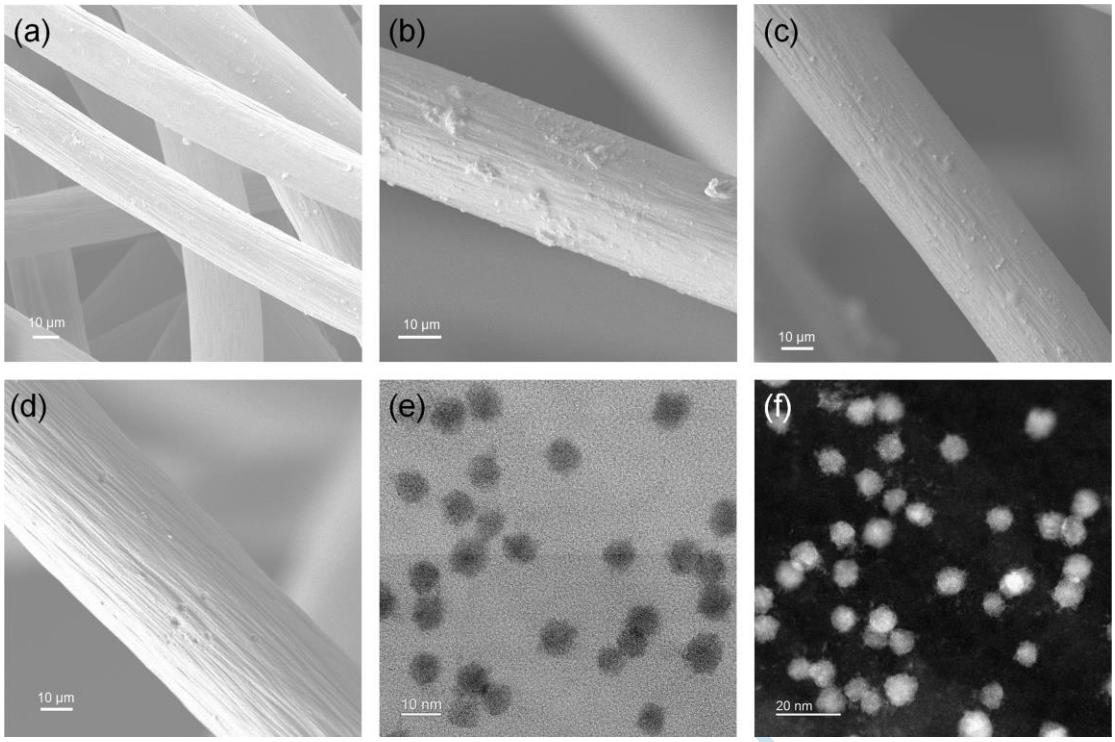

Fig. S1. SEM images of (a) GF, (b) Bi/N-GF, (c) N-GF, and (d) Bi-GF. (e and f) High-magnification (e) TEM and (f) STEM images of Bi/N-GF.

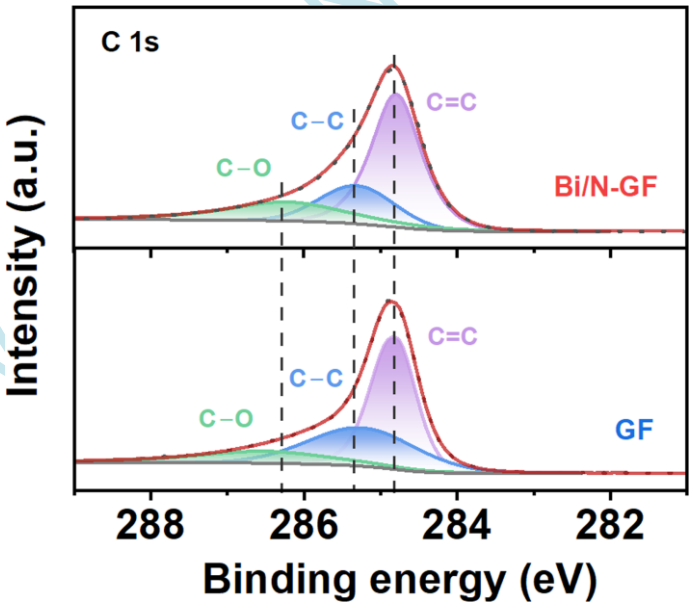

Fig. S2. C 1s XPS spectra of GF and Bi/N-GF.

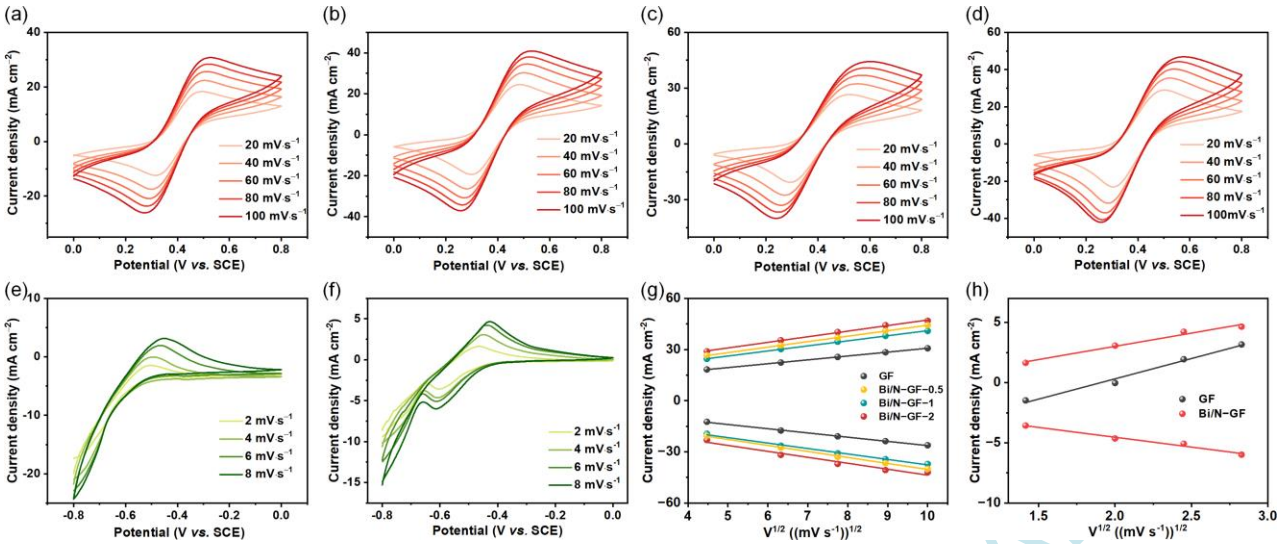

Fig. S3. CV curves of (a) GF, (b) Bi/N-GF_0.5, (c) Bi/N-GF_1, and (d) Bi/N-GF_2 in 1.0 M $FeCl_2 \cdot 4H_2O$ + 1.0 M $CrCl_3 \cdot 6H_2O$ + 3.0 M HCl solution by varying the scan rate from 20.0 to 100.0 mV s^{-1} and voltage range of 0.0 ~ 0.8 V (*vs.* SCE). CV curves of (e) GF and (f) Bi/N-GF_2 in 1.0 M $FeCl_2 \cdot 4H_2O$ + 1.0 M $CrCl_3 \cdot 6H_2O$ + 3.0 M HCl solution by varying the scan rate from 2.0 to 8.0 mV s^{-1} and voltage range of −0.8 ~ 0.0 V (*vs.* SCE). (g) Variation curves of Fe^{2+}/Fe^{3+} peak current density (top: oxidation current; bottom: reduction current) of GF, Bi/N-GF_0.5, Bi/N-GF_1, and Bi/N-GF_2 as a function of the square root of sweep speed. (h) Variation curves of Cr^{3+}/Cr^{2+} peak current density of GF and Bi/N-GF (top: oxidation current; bottom: reduction current) versus the square root of sweep speed.

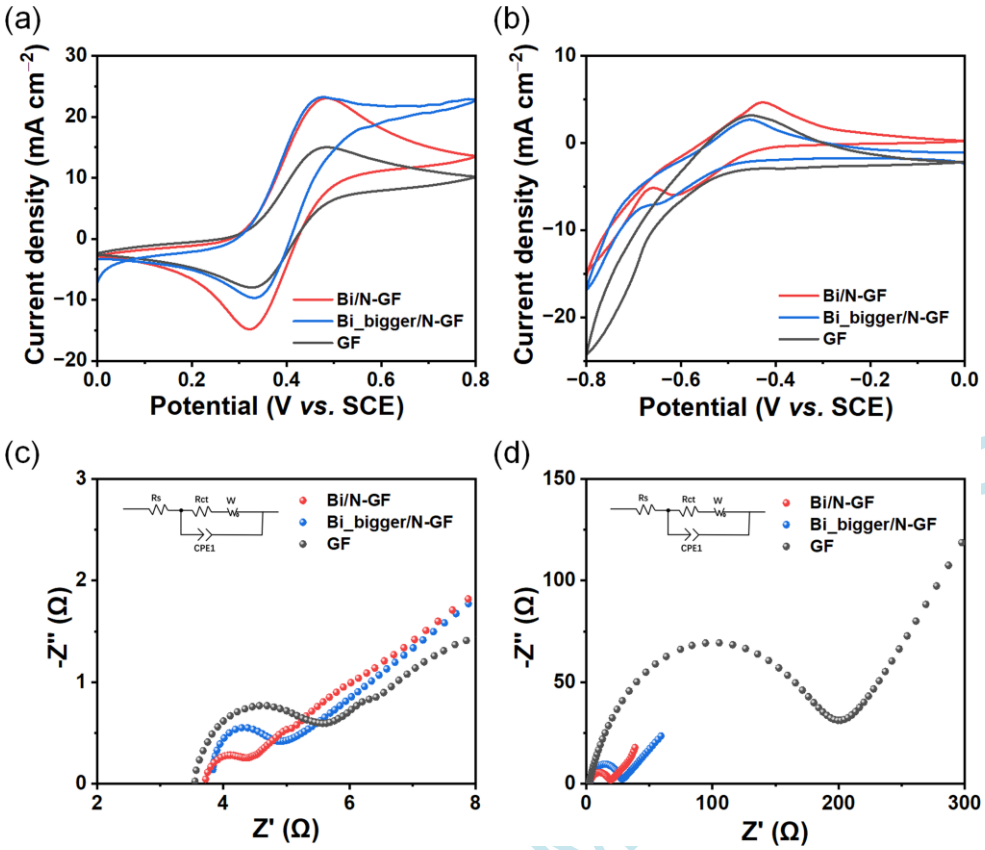

Fig. S4. CV curves of Bi/N-GF, Bi_bigger/N-GF, and GF derived under a scan rate of (a) 10.0 mV s^{-1} and voltage range of 0.0−0.8 V (*vs.* SCE) at the positive electrode and (b) 8.0 mV s^{-1} and voltage range from −0.8 to 0.0 V (*vs.* SCE) at the negative electrode. EIS diagrams of Bi/N-GF, Bi_bigger/N-GF, and GF measured under (c) 0.35 V (*vs.* SCE) at the positive electrode and (d) −0.5 V (*vs.* SCE) at the negative electrode.

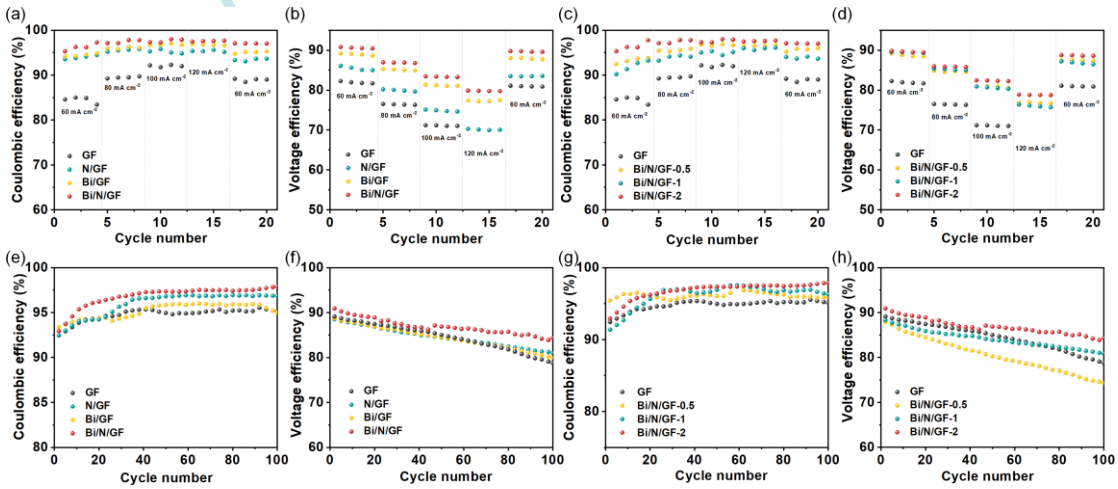

Fig. S5. (a and e) CE and (b and f) VE of GF, N-GF, Bi-GF, and Bi/N-GF at different current densities in ICRFBs. (c and g) CE and (d and h) VE of GF, Bi/N-

GF_0.5, Bi/N-GF_1, and Bi/N-GF_2.0 at 60.0 mA cm^{-2} and 100 cycles in ICRFB.

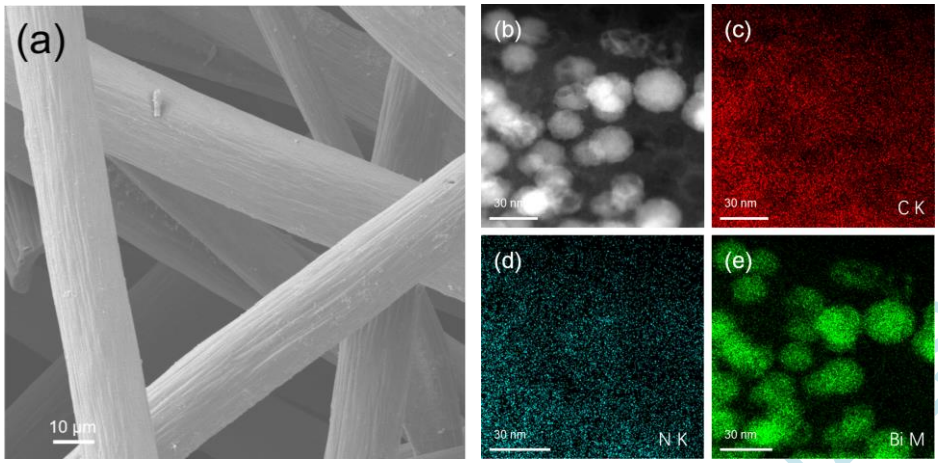

Fig. S6. (a) SEM, (b) STEM and (c−e) accompanying EDS mapping images of Bi/N-GF after electrochemical cycling tests at different current densities.

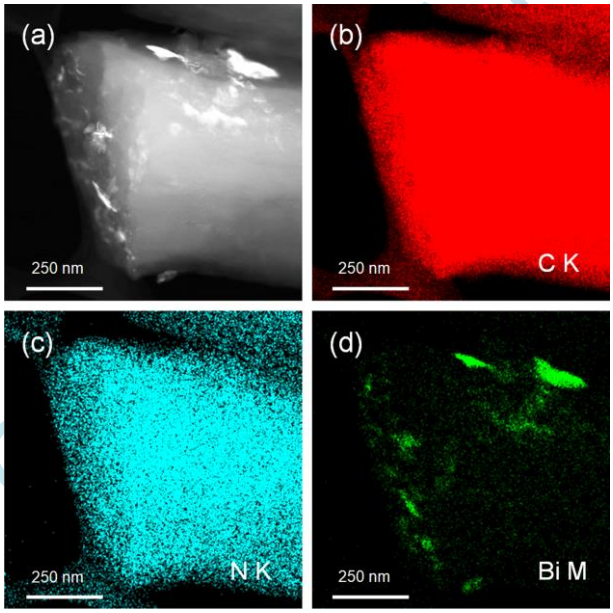

Fig. S7. (a) STEM and (b−d) EDS mapping images of Bi_bigger/N-GF. From the STEM image, big Bi aggregates are discerned.

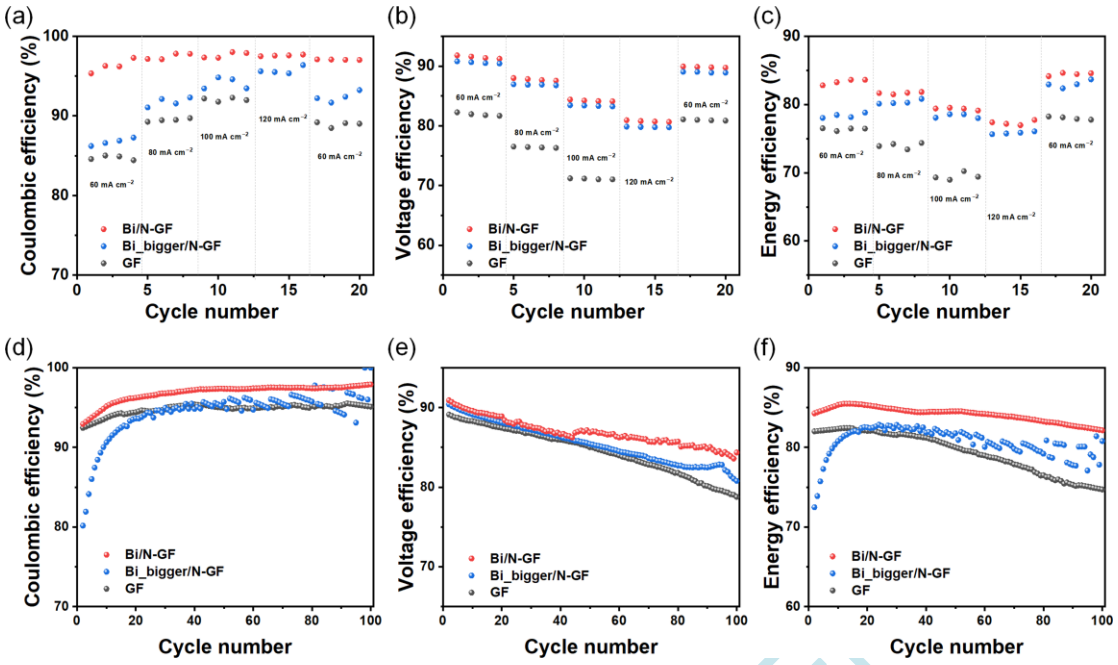

Fig. S8. (a) CE, (b) VE, and (c) EE of Bi/N-GF, Bi_bigger/N-GF, and GF at different current densities in ICRFBs. (d) CE, (e) VE, and (f) EE of Bi/N-GF, Bi_bigger/N-GF, and GF at 60.0 mA cm^{-2} and 100 cycles in ICRFBs.

Table S1. CV electrochemical data of GF, Bi/N-GF, N-GF, and Bi-GF in 1.0 M $FeCl_2·4H_2O$ + 1.0 M $CrCl_3·6H_2O$ + 3.0 M HCl solution, with a scanning rate of 40.0 mV s^{-1} and voltage range of 0.0 ~ 0.8 V (*vs.* SCE).

Sample	E_{pa} / V	I_{pa} / mA cm^{-2}	E_{pc} / V	I_{pc} / mA cm^{-2}	ΔE / V	$-I_{pa}$ / I_{pc}
GF	0.50	22.37	0.30	−17.47	0.20	1.28
Bi/N-GF	0.53	35.42	0.26	−32.49	0.27	1.09
N-GF	0.52	18.65	0.28	−13.75	0.25	1.36
Bi-GF	0.45	33.41	0.22	−30.41	0.22	1.12

Table S2. CV electrochemical data of GF, Bi/N-GF, N-GF, and Bi-GF in 1.0 M $FeCl_2·4H_2O$ + 1.0 M $CrCl_3·6H_2O$ + 3.0 M HCl solution, with a scanning rate of 6.0 mV s^{-1} and voltage range of −0.8 ~ 0.0 V (*vs.* SCE).

Sample	E_{pa} / V	I_{pa} / mA cm^{-2}	E_{pc} / V	I_{pc} / mA cm^{-2}	ΔE / V	$-I_{pa}$ / I_{pc}
GF	−0.47	1.95	/	/	/	/
Bi/N-GF	−0.44	4.23	−0.61	−5.07	0.18	0.83
N-GF	−0.46	3.57	/	/	/	/
Bi-GF	−0.38	2.27	/	/	/	/

Table S3. CV electrochemical data of GF, Bi/N-GF_0.5, Bi/N-GF_1, and Bi/N-GF_2 in 1.0 M $FeCl_2·4H_2O$ + 1.0 M $CrCl_3·6H_2O$ + 3.0 M HCl solution, with a scanning rate of 40.0 mV s^{-1} and voltage range of 0.0 ~ 0.8 V (*vs*. SCE).

Sample	E_{pa} / V	I_{pa} / mA cm^{-2}	E_{pc} / V	I_{pc} / mA cm^{-2}	ΔE / V	$-I_{pa}$ / I_{pc}
GF	0.50	22.37	0.30	−17.47	0.20	1.28
Bi/N-GF_0.5	0.55	32.35	0.27	−27.45	0.28	1.18
Bi/N-GF_1	0.50	30.25	0.28	−26.42	0.22	1.15
Bi/N-GF_2	0.52	35.42	0.29	−32.49	0.24	1.09

Table S4. CV electrochemical data of GF, Bi/N-GF_0.5, Bi/N-GF_1, and Bi/N-GF_2 in 1.0 M $FeCl_2·4H_2O$ + 1.0 M $CrCl_3·6H_2O$ + 3.0 M HCl solution, with a scanning rate of 6.0 mV s^{-1} and voltage range of −0.8 ~ 0.0 V (*vs*. SCE).

Sample	E_{pa} / V	I_{pa} / mA cm^{-2}	E_{pc} / V	I_{pc} / mA cm^{-2}	ΔE / V	$-I_{pa}$ / I_{pc}
GF	−0.47	1.95	/	/	/	/
Bi/N-GF_0.5	−0.48	3.18	−0.61	−6.76	0.13	0.43
Bi/N-GF_1	−0.45	4.84	−0.63	−9.72	0.19	0.50
Bi/N-GF_2	−0.44	4.23	−0.61	−5.07	0.16	0.83

Table S5. EIS electrochemical data of GF, Bi/N-GF, N-GF, and Bi-GF in 1.0 M $FeCl_2·4H_2O$ + 1.0 M $CrCl_3·6H_2O$ + 3.0 M HCl solution. The polarization voltages are 0.35 V (*vs*. SCE) and −0.5 V (*vs*. SCE).

	0.35 V				−0.5 V			
Sample	GF	Bi/N-GF	N-GF	Bi-GF	GF	Bi/N-GF	N-GF	Bi-GF
R_{ct}/Ω	1.25	0.02	0.14	0.32	190.80	15.65	55.99	37.03
R_s/Ω	3.69	3.48	3.86	3.95	2.72	2.36	2.19	2.67

Table S6. EIS electrochemical data of GF, Bi/N-GF_0.5, Bi/N-GF_1, and Bi/N-GF_2 in 1.0 M $FeCl_2·4H_2O$ + 1.0 M $CrCl_3·6H_2O$ + 3.0 M HCl solution. The polarization voltages are 0.35 V (*vs*. SCE) and −0.5 V (*vs*. SCE).

	0.35 V				−0.5 V			
Sample	GF	Bi/N-GF_0.5	Bi/N-GF_1	Bi/N-GF_2	GF	Bi/N-GF_0.5	Bi/N-GF_1	Bi/N-GF_2

R_{ct}/Ω	1.25	0.77	0.41	0.02	190.80	21.44	27.42	15.65
R_s/Ω	3.69	4.38	4.46	3.48	2.72	2.62	2.01	2.36